Journal of Petroleum Research and Studies

Open Access
No. 34 part 2, April 2022, pp. 18-34

P- ISSN: 2220-5381
E- ISSN: 2710-1096

DOI: http://doi.org/10.52716/jprs.v12i1(Suppl.).618

Geological Study for the Outbreak of Fires Phenomenon in Al-Ruhban Oasis, An-Najaf Al-Ashraf

Ali H. Hejooj and Haider Ahmed Falih Al-Tarim*
Oil Exploration Company- Ministry of Oil
*Corresponding Author E-mail: haiderafalih@gmail.com, oecman@oec.oil.gov.iq

6th Iraq Oil and Gas Conference, 29-30/11/2021

Abstract

The current study focused on the phenomenon of the outbreak of fires and their causes in Al-Ruhban Oasis in terms of geologically, its economic importance and its environmental dimensions from the point of view of the Oil Exploration Company, depending on geological and geophysical information, laboratory analyzes and geochemical surveys that were carried out at the site of the phenomenon and the surrounding areas.

The region was affected by major normal fault systems that reach the surface, that this type of fault reflects the region's influence by structural forces represented by the vertical lifting movements of the basement dislocation, in addition to the marking of secondary faults that affected the shallow reflectors, and that these faults the secondary reflects that the region has been affected by other structural forces that have reactivated the old faults.

Laboratory analyzes of soil samples at the site of the phenomenon and the surrounding areas indicated a clear discrepancy in the amount of pollution, as the surface samples recorded very little percentages compared to the subsurface samples that recorded the highest pollution values, where the highest values of hydrocarbon pollution were recorded, which indicates that hydrocarbon emissions have relatively deep subsurface source and that they are not only caused by surface pollution effects. Migratory hydrocarbon emissions from effective source rocks in the region or from potential oil and/or gas accumulation in the region is one of the most important causes of fires in the Oasis of Al-Ruhban and is a direct indication of hydrocarbon potentialities in the area.

Keywords: Geological study, Phenomenon of fires, Al-Ruhban Oasis, Al-Najaf Al-Ashraf.

1. Introduction

During the exploration history within the Najaf governorate, 40 structural leads were identified a potential hydrocarbon trap and three exploration wells were drilled, oil has

Open Access
No. 34 part 2, April 2022, pp. 18-34

P- ISSN: 2220-5381
E- ISSN: 2710-1096

discovered within the Zubair and Nahr Umr formations in the Kifl oil field with an initial hydrocarbon in place of 500 million barrels, of which 128 million barrels can be produced, as for the Ghlisan and Safawi structures, the results of exploratory drilling indicated that they were dry at the level of the penetrated formations[1].

Geographical location Al-Ruhban Oasis is approximately 45 km to the west of the city center of Najaf governorate (Figs.1and 2), within Al Tar archaeological area near the Najaf Sea. The area is one of the fault shear zones located west of the Euphrates River between the governorates of Anbar, Karbala and Najaf, as it descends towards the south within the fault zone of Abu Jir and within caves and valleys, this area is believed to be rich in minerals. Table (1) shows the coordinates of the two fire areas in Al-Ruhban area and shows the area of the current study that dealt with the interpretation of the phenomenon according to the global coordinate system U.T.M WGS, 1984 ZONE 38.

Table (1) Coordinate of the study area

Point	X Coor.	Y Coor.
A	379632	3580205
B	440084	3580339
C	440084	3508010
D	379899	3507877

The current study aims to examine the phenomenon of the outbreak of fires and their causes in Al-Ruhban Oasis in terms of geologically, its economic importance and its environmental impacts from the point of view of the Oil Exploration Company, depending on geological and geophysical information, laboratory analyzes and geochemical surveys that were carried out at the site of the phenomenon and the surrounding areas.

Open Access
No. 34 part 2, April 2022, pp. 18-34

P- ISSN: 2220-5381
E- ISSN: 2710-1096

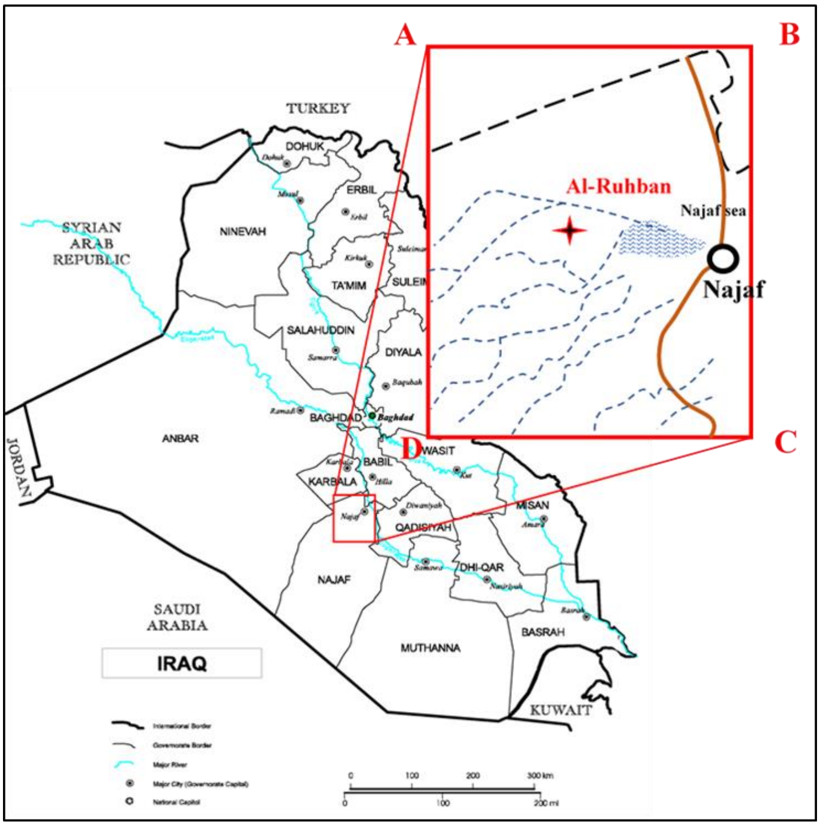

Fig. (1): The administrative map of Iraq showing the location of the Al-Ruhban Oasis [2]

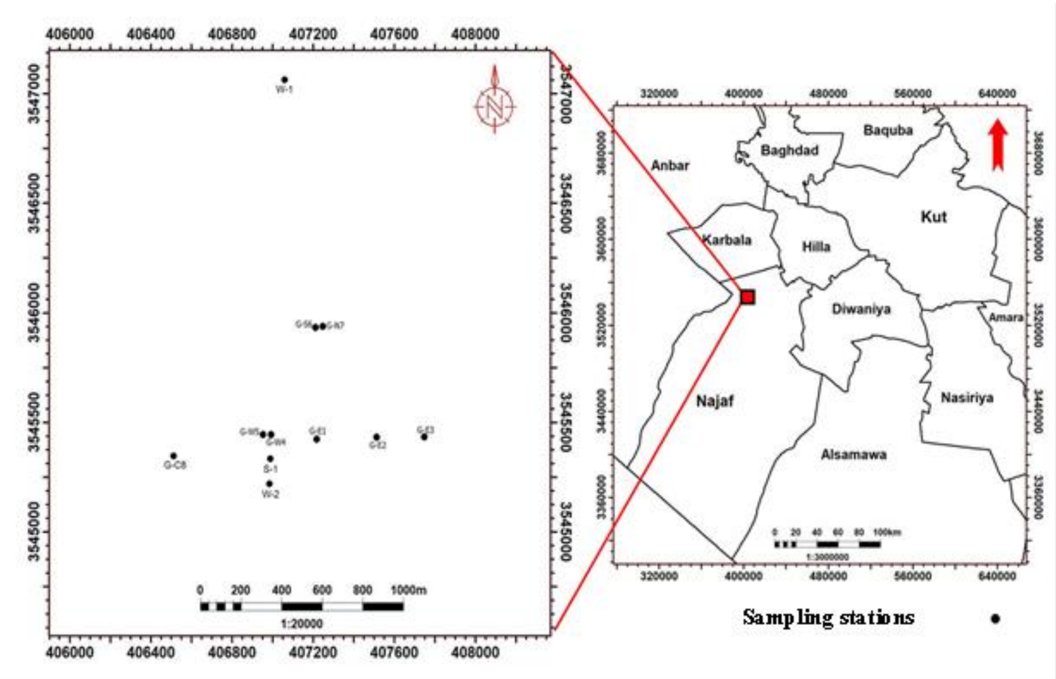

Fig. (2): Location map showing the locations of sampling collection.

Open Access
No. 34 part 2, April 2022, pp. 18-34

P- ISSN: 2220-5381
E- ISSN: 2710-1096

2. Material and Methods

2.1 Exploratory geophysical data

The area of study was included in a number of seismic interpretive studies, where the structural maps of these studies showed that the Al-Kifl oil field borders the Al-Ruhban area from the northeastern side with a distance of 17 km, knowing that the wells of the field produce oil from the Zubair and Nahr Umr formations, and the area is bounded by a Sura structure from the northwest side with a distance of 15 km, as in Figure (3) represents a time map of the Shuaiba reflector on which is located a Sura structure and the location of the Al-Ruhban Oasis phenomenon.

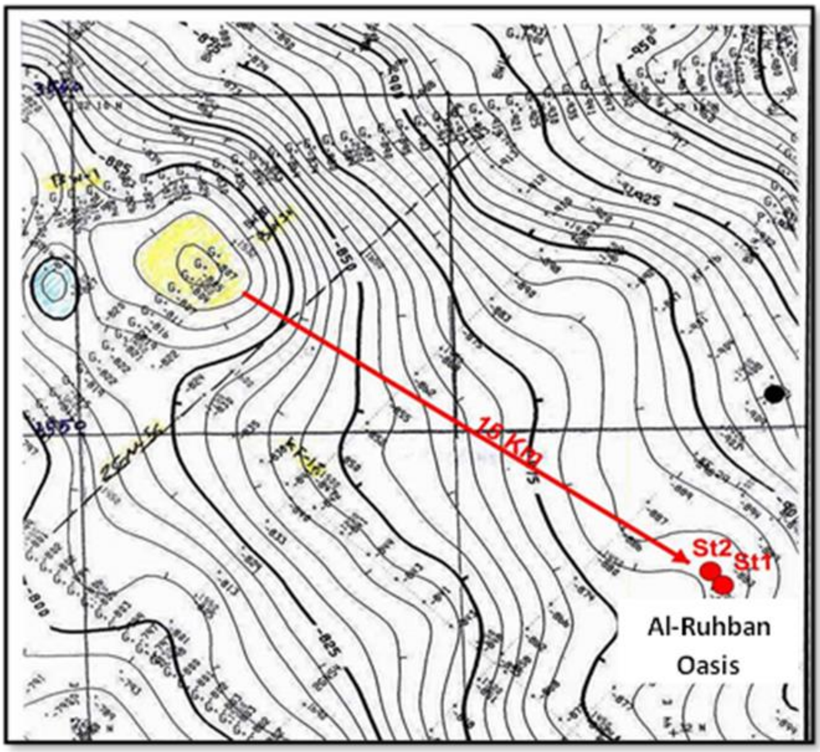

Fig. (3): A time map of the Shuaiba reflector shows the distance between Sura structure and the Al-Ruhban Oasis phenomenon [1].

2.2 Laboratory Tests

Surface soil samples were collected at a depth of 0.5 m and along the bore of a well in the area of occurrence the phenomena, which has been drilled for a total depth of 20 m and at a sampling rate of 1.5 meters. Two water samples from the depths confined between 18-20 meters from the aforementioned well. Quantitative and qualitative tests of gases were

Open Access
No. 34 part 2, April 2022, pp. 18-34

P- ISSN: 2220-5381
E- ISSN: 2710-1096

conducted for the purpose of determining the presence of gases emitted from 8 measurements stations, 7 of them at the site of the phenomenon, and station 8 is 0.5 km away from the site. Table (2) coordinate of samples collection position and Figure (4) a map illustrated these locations.

Table (2) Coordinates of the sampling sites.

Station No.	Easting	Northing
Soil sample		
S1	407001.00	3545346.00
Water Sample		
W1	407049.00	3547055.00
Gas Station		
G-East 1	407001.00	3545346.00
G-East 2	407030.13	3545346.86
G-East 3	407053.93	3545347.81
G-West 4	406977.18	3545347.97
G-West 5	406951.07	3545348.00
G-South 6	407000.45	3545294.18
G-North 7	407001.13	3545394.65
G-Center 8	406509.54	3545350.15

3. Results of Seismic Data

The results of the 3D seismic data interpretation in the Merjan oil field West-Kifl area, which were implemented by OEC team work in 2012[3], showed that there are several possible places for gas presence in the region, which were not previously indicated by 2D seismic data of the, Figure (3).

Open Access
No. 34 part 2, April 2022, pp. 18-34

P- ISSN: 2220-5381
E- ISSN: 2710-1096

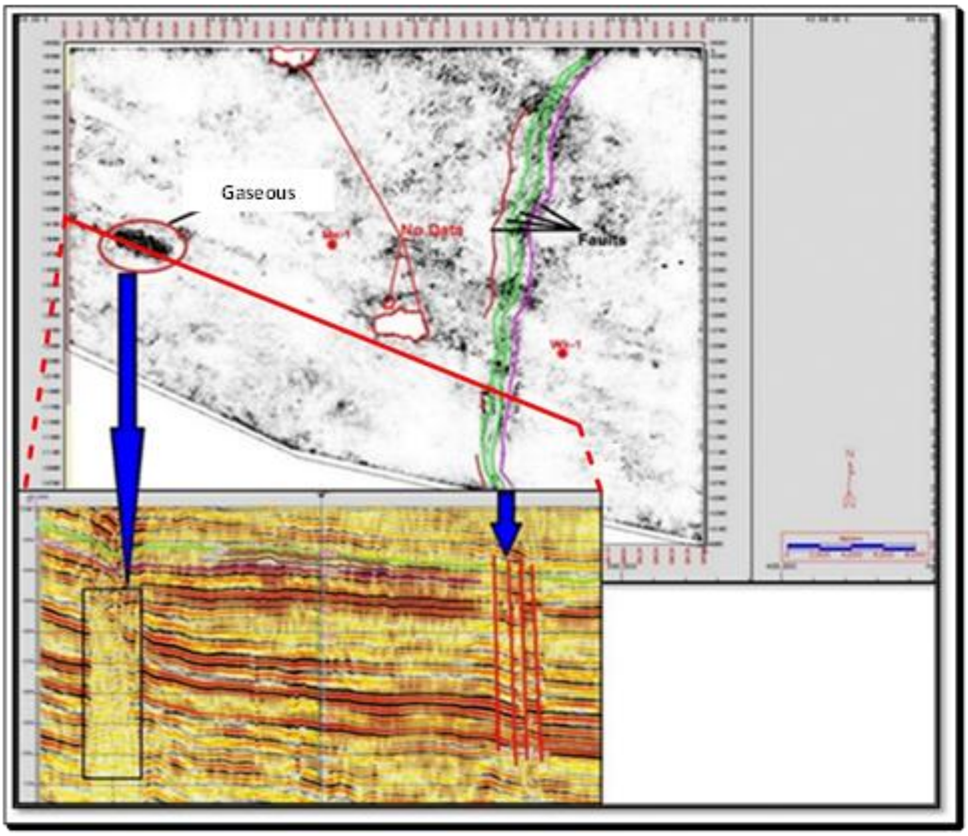

Fig. (4): Axial seismic section showing the effect of a seismic function that reflects the presence of gas in the Marjan region West of Al-Kifl [3]

In the present study, there are 17 2D migrated seismic lines belonging to the Kifl survey covering the location of Al-Ruhban phenomenon and its surrounding extensions were downloaded, and through the process of examining and reviewing seismic data, the quality of the seismic reflectors ranged from weak to medium in relation to the level of interset. Which represents the formations of Al-Hartha and Al-Mishrif / Rumaila, and good quality for the reflector at the level of Zubair Formation. Figure (5) represents a base map showing the paths of the seismic lines that were used in the current study. The map also shows that the seismic line (Kf-20) passes through the site of the phenomenon at the shoot point 1400, Figure (6).

Open Access
No. 34 part 2, April 2022, pp. 18-34

P- ISSN: 2220-5381
E- ISSN: 2710-1096

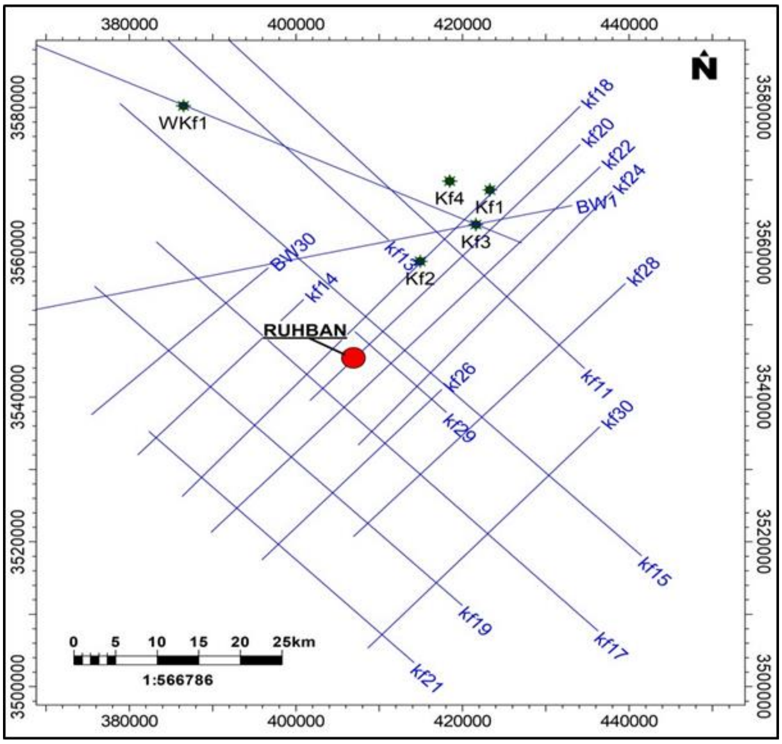

Fig. (5): A basic map showing the paths of the seismic lines covering the location of Al-Ruhban phenomenon and the locations of the wells of the Al-Kifl oil field.

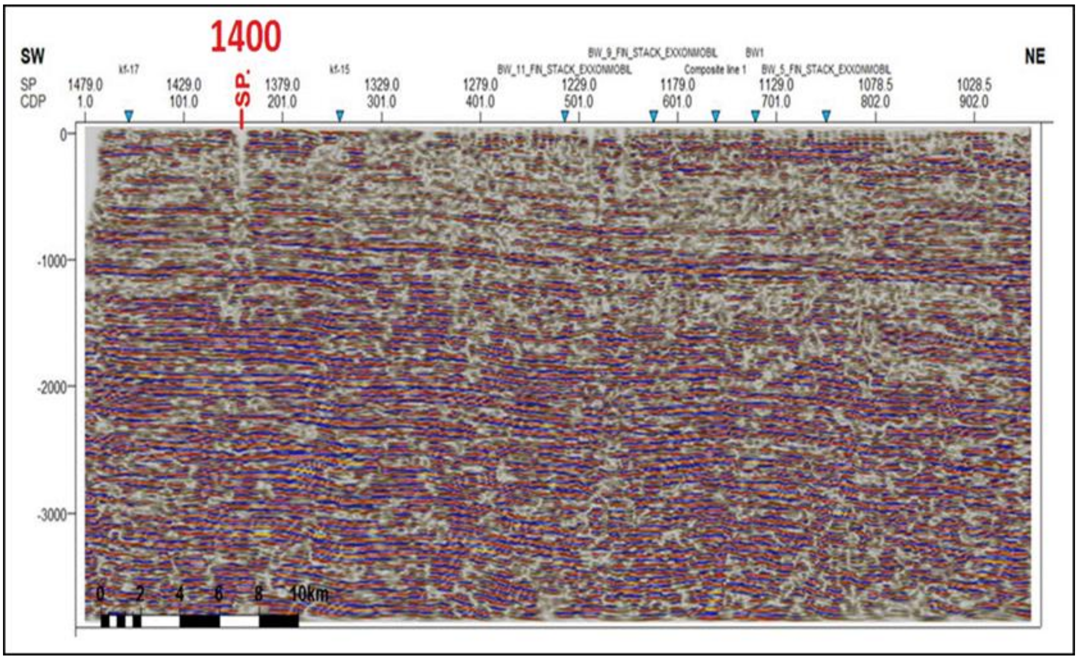

Fig. (6): Dip direction Seismic Line KF-20 the location of the phenomenon at the shoot point of 1400.

Open Access
No. 34 part 2, April 2022, pp. 18-34

P- ISSN: 2220-5381
E- ISSN: 2710-1096

3.1 Interpretation of fault systems

The process of capturing and tracking the reflector, which represents the top of the Zubair Formation, was carried out on the two-dimensional seismic data and traced the affecting faults in the region and determined their type, where the main and secondary faults were marked. This type of fault reflects the region's being affected by structural forces represented by the vertical lifting movements of the basement dislocation, in addition to the indication of secondary faults that affected the shallow deflectors, and that these secondary faults reflect that the region has been affected by other structural forces that reactivate the old faults. It is concluded that it difficult to represent and draw the boundaries of the fault zones on the map because the region has been affected by more than one rifting system, Figures (7).

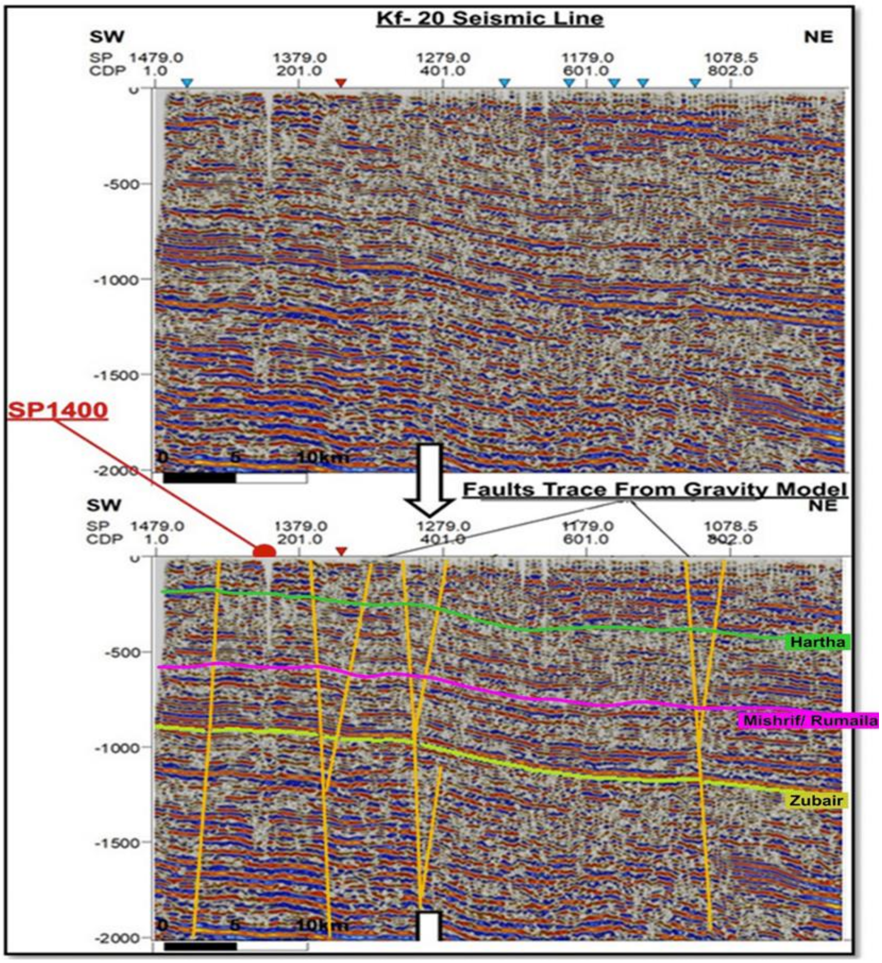

Fig. (7): Seismic section of the dipping line Kf-20 showing the process of marking the faults and tracking the reflector of the Zubair Formation.

Open Access
No. 34 part 2, April 2022, pp. 18-34
P- ISSN: 2220-5381
E- ISSN: 2710-1096

Therefore, in order to reach the optimal model of the structural image in the region and to know the type of faults affecting it, it was found necessary to integrate with the data of the gravitational map. Derivation processes to the horizontal and vertical covariance of the values of the residual gravity and elicit the values of the slope phase for these values for the purpose of indicating the fault paths affecting the region according to the two equations below [4]:

TDR = tan-1[VDR/THDR] ……………………………………1

THDR = √(∂A/∂x)2+(∂A/∂y)2…………………………………….2

Local wavenumber = TDR to THDR

TDR: Tilt Derivative

VDR: Vertical Derivative

THDR: Total horizontal Derivative

By applying the mechanism mentioned in the gravitational derivation, the milling phase values were deduced and a map of the horizontal variation in the gravitational values was drawn from the level of the ancient formations, which more accurately illustrates the paths and fault systems. North-south direction that mainly affected the region, a longitudinal fault system taking a northwest-southeast direction affected the northern parts of the region, and a transverse fault system taking a northeast-southwest direction which changed the direction of the axes of the older structures and fault systems.

3.2 Structured model and depth map output

The faults deduced from the gravitational milli-phase map were entered into the seismic interpretation project and matched with the seismic data capture results for seismic survey lines, especially on the seismic section (Kf-20) that passes at the site of Al-Ruhban phenomenon. Existing on the seismic sections used in the current study, in light of this, a three-dimensional structural model of the faults plans was made in the study area and the temporal surfaces representing the reflectors of Haritha, Mishrif / Rumaila and Zubair were made, and then a three-dimensional structural model was prepared between the Faults systems and time surfaces according to equal and complementary standards that lead to building structural skeleton that reflect the results of tracking seismic reflectors and identifying different fault systems and prepared for volumetric

Open Access
No. 34 part 2, April 2022, pp. 18-34

P- ISSN: 2220-5381
E- ISSN: 2710-1096

calculations and petrophysical distribution using the application (Structural Griding) in the work project available in the Peterl program and thus outputting the time maps of the above reflectors and converting to depth maps using velocity Regional average of surrounding wells (Fig. 8).

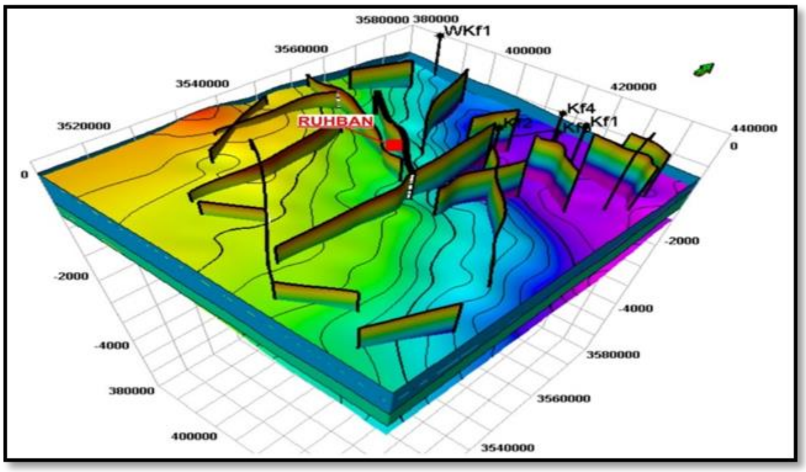

Fig. (8): The three-dimensional model in the depth field showing the location of Al-Ruhban phenomenon.

4. Results of Geochemical Data

Table (3) shows that the water analysis of three samples taken from artesian well, 1.7 km away from the study area do not indicate hydrocarbon pollution, as they focus on the physical and chemical properties of water, so it has been decided to use the ERACHECK ECO device, which is highly effective in determining minor concentration of hydrocarbon pollution.

Table (3) Results of water tests for an artesian well 1.7 km from the study area

W1	T.D.S ppm	SO_4 ppm	HCO_3 ppm	Cl ppm	Ca ppm	Mg ppm	Na ppm
1	662	128	61	142	25	12	294
2	660	126	63	142	24	17	290
3	666	130	61	142	24	15	294

The values of (TPH) (2.1-13) mg/L, Table (4), showed a high percentage of hydrocarbon pollution for two water samples at a depth of (18 and 20) meters.

Table (4) Results of TPH Tests in Water

TPH mg/L	Sample Depth m	Test
2.1	18	Total Petroleum Hydrocarbons
13	20	

Open Access
No. 34 part 2, April 2022, pp. 18-34

P- ISSN: 2220-5381
E- ISSN: 2710-1096

For the purpose of studying the amount of organic matter in the surface and subsurface soil samples, the technique of thermal cracking of rocks in isolation from air (Pyrolysis) was used using the Rock-Eval 6 device, usually to identify several geochemical factors of the rock.

Through the results of the analysis of the surface and subsurface rock models in Tables (5) and (6), it was found that the rock sampled contain varying percentages of organic materials ranging between (0.41-7.83) % of the weight of the rock, and this indicates that the area contains organic materials that has been generated from the remains of the roots of plants being an agricultural area. As for the free hydrocarbons, they are inferred from the recording of (S1) readings. It is noticeable that they are not recorded in most of the analyzed models except for the two samples (2, 6), whose ratio is (0.41, 0.13) respectively, which is a very few or poor percentage according to the standard of Geochemical parameters of [5] and to find out the origin of these few percentages of released hydrocarbons, the values of (S1, TOC) were represented in Figure (9) on the graph of the relationship between them to show that the presence of very few percentages of hydrocarbons is mostly the result of high temperature Heat of surface rocks containing plant organic matter based on the values of the hydrogen index (HI) according to the geochemical criteria [5], which are considered values between (50-200) as an indicator of plant organic matter, and values less than 50 are indicative of organic matter. Inactive membership.

Table (5) Thermal Fracture Analysis of Surface Soil Models (Pyrolysis) Using Rock-Eval-6.

Sample No.	S1	S2	S3	HI	OI	PI	PP	Tmax	PC	RC	TOC Wt%	Min C Wt%
1	0	0	0.01	0	7	0	0	607	0	0	0	0
2	0.41	5.23	4.3	136	112	0.07	5.64	444	0.7	0.7	0.7	0.7
3	0	0.14	1.24	15	135	0	0.14	483	0.06	0.06	0.06	0.06
4	0	0.3	0.05	103	17	0	0.3	608	0.03	0.03	0.03	0.03
5-a	0	0.28	0.17	35	21	0	0.28	608	0.04	0.04	0.04	0.04
5-b	0	0.25	2.1	3	27	0	0.25	531	0.21	0.21	0.21	0.21
6	0.13	0.3	0.71	37	88	0.3	0.43	361	0.07	0.07	0.07	0.07

Open Access
No. 34 part 2, April 2022, pp. 18-34

P- ISSN: 2220-5381
E- ISSN: 2710-1096

Table (6) Thermal Fracture Analysis of Subsurface Soil Models (Pyrolysis) by Rock-Eval-6

Depth m	S1	S2	S3	HI	OI	PI	PP	Tmax	PC	RC	TOC Wt%	MinC Wt%
12 m	0	0.02	0.13	200	1300	0	0.02	450	0.01	0	0.01	3.5
13.5 m	0	0	0.07	0	0	0	0	449	0	0	0	3.71

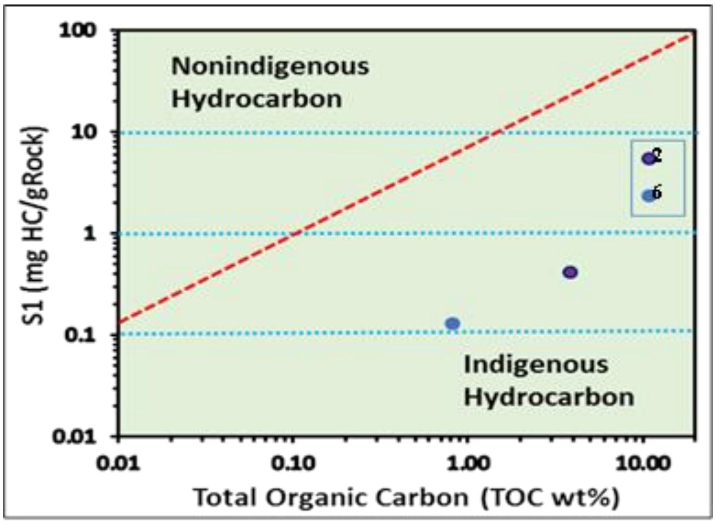

Fig. (9): The relationship between S1 Vs TOC

As for the soil samples taken from different depths for TPH analyzes, it was shown in Table (7), which were (12) soil samples, that they ranged between (63-18464) mg/L, which is higher than its value in water, with no values recorded for four samples.

Table (7) Results of TPH tests in the surface and subsurface soils.

TPH mg/L	Sample Depth m	Test
25	Surface Sample 1	Total Petroleum Hydrocarbons
11	Surface Sample 2	
7771	2	
1073	3.5	
1278	5	
ND	6.5	
1359	9.5	
3953	11	
18464	12	
14049	13.5	
ND	15.5	
ND	17	
ND	18	
63	20	

Open Access
No. 34 part 2, April 2022, pp. 18-34

P- ISSN: 2220-5381
E- ISSN: 2710-1096

As for the soil samples taken from the depths of the drilled well, which is 20 meters deep near the phenomena site, the laboratory results of TPH analyzes of surface and subsurface soil models at depths ranging from 0.5 meters to 20 meters were found. Compared to the subsurface models that recorded higher pollution values, while the two samples at a depth of 12 and 13 meters recorded the highest pollution values in the soil, which is considered contaminated with hydrocarbon. Figure (10) shows the concentration of TPH with the depth that shows the contamination of samples with BTEX materials compared to the surface samples.

Gasmet device was used to diagnose the gases emitted in Al-Rahaban Oasis area, where the gases were identified in 8 stations. The results of the examination of the stations indicated the presence of the following gases (Carbon dioxide, Carbon monoxide, Nitrous oxide, Methane, Ethane, Ethylene, M-Xylene, O-Xylene, Phenol, Furan, Hydrogen cyanide, Ammonia, Hydrogen chloride, Hydrogen fluoride, Nitrogen dioxide, Sulfur dioxide) [6], which somewhat corresponds to the gases known in the gas reservoirs and which are shown in Table (8), where we will review the results for the gas testing stations from the G-East1 station to the G-Center8 station.

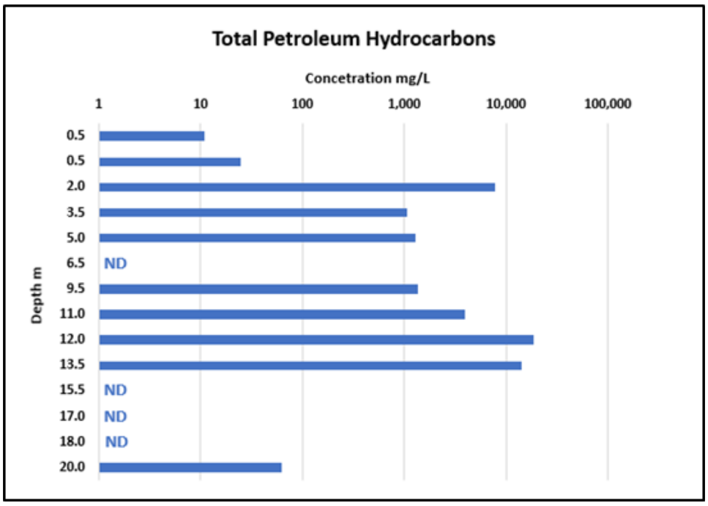

Fig. (10): The distribution of TPH concentrations with depth

Open Access
No. 34 part 2, April 2022, pp. 18-34

P- ISSN: 2220-5381
E- ISSN: 2710-1096

Table (8) Results of Gas Tests for G-East 1

Range	Compensation	Unit	Concentration	Component	Chamber
3	wet	vol-%	0.89	Water vapor	1
2000	wet	ppm	402.01	Carbon dioxide	2
200	wet	ppm	0.00	Carbon monoxide	3
100	wet	ppm	0.21	Nitrous oxide	4
100	wet	ppm	1.83	Methane	5
200	wet	ppm	0.29	Ethane	6
200	wet	ppm	0.54	Ethylene	7
50	wet	ppm	0.20	Benzene	8
200	wet	ppm	0.00	Toluene	9
200	wet	ppm	0.00	M-Xylene	10
200	wet	ppm	0.32	O-Xylene	11
100	wet	ppm	0.00	P-Xylene	12
50	wet	ppm	0.00	Naphthalene	13
50	wet	ppm	0.00	Phenol	14
200	wet	ppm	0.16	Furan	15
50	wet	ppm	0.23	Hydrogen cyanide	16
200	wet	ppm	0.00	Ethyl chloride (chloroetha...	17
200	wet	ppm	0.00	Chlorobenzene (Phenyl c...	18
50	wet	ppm	0.20	Ammonia	19
50	wet	ppm	0.07	Hydrogen chloride	20
50	wet	ppm	0.02	Hydrogen fluoride	21
50	wet	ppm	0.00	Nitrogen dioxide	22
100	wet	ppm	0.19	Sulfur dioxide	23
1150	N/A	mbar	1020.00	Ambient pressure	1201
40	N/A	°C	27.00	Cell temperature	1202

For the purpose of verifying that the gases emitted in the study area are gases emitted from reservoirs containing hydrocarbon, and using the Gasmet device, results were searched for gas tests that were carried out by the same device for one of the oil and/or gas reservoirs in the neighboring areas. These results were not found, so gas models were used. They were collected in special containers from the Khasib, Mishrif and Zubair reservoirs of an exploratory well which was newly drilled and relatively far away. It was found that there is a perfect match between the gases diagnosed in the area of the Al Ruhban area and the gases measured in the exploratory well, Table (9).

Open Access
No. 34 part 2, April 2022, pp. 18-34

P- ISSN: 2220-5381
E- ISSN: 2710-1096

Table (9) Results of gas tests for the Zubair Formation in the exploratory well.

Range	Compensation	Unit	Concentration	Component	Chamber
3	wet	vol-%	1.44	Water vapor	1
2000	wet	ppm	1645.91	Carbon dioxide	2
200	wet	ppm	68.83	Carbon monoxide	3
100	wet	ppm	0.03	Nitrous oxide	4
100	wet	ppm	17.12	Methane	5
200	wet	ppm	2.54	Ethane	6
200	wet	ppm	0.92	Ethylene	7
50	wet	ppm	1.47	Benzene	8
200	wet	ppm	0.00	Toluene	9
200	wet	ppm	0.00	M-Xylene	10
200	wet	ppm	1.06	O-Xylene	11
100	wet	ppm	0.00	P-Xylene	12
50	wet	ppm	0.00	Naphthalene	13
50	wet	ppm	0.28	Phenol	14
200	wet	ppm	0.88	Furan	15
50	wet	ppm	3.23	Hydrogen cyanide	16
200	wet	ppm	0.00	Ethyl chloride (chloroetha...	17
200	wet	ppm	0.00	Chlorobenzene (Phenyl c...	18
50	wet	ppm	10.16	Ammonia	19
50	wet	ppm	0.51	Hydrogen chloride	20
50	wet	ppm	0.02	Hydrogen fluoride	21
50	wet	ppm	0.00	Nitrogen dioxide	22
100	wet	ppm	0.00	Sulfur dioxide	23
1150	N/A	mbar	1021.00	Ambient pressure	1201
40	N/A	°C	27.00	Cell temperature	1202

5. Conclusions

1. The region was affected by major fault systems of normal type that reach the surface, the types and natures of faults indicate that the region's influence by structural defomation represented by the vertical lifting movements of the basement dislocation, in addition to conclude of secondary faults system that affected the shallow deflectors, The presences of secondary deformation reflects that the region has been affected by other tectonic forces lead to reactivated the preexisting faults.
2. The general structural slope ranges from the southwestern side (the highest structurally) to the eastern and northeastern side (the lowest structurally) for all geological formations from the ancient to the modern geological era.
3. The tectonic deformation caused lead to deterioration of seismic signal and this was confirmed by the processing and interpretation of gravitational data through a clear change in the anomalies axes of the phenomenon region.

Open Access
No. 34 part 2, April 2022, pp. 18-34

P- ISSN: 2220-5381
E- ISSN: 2710-1096

4. The absence of a structural closure at the site of the phenomenon is considered one of the most risky factor for exploration drilling and the main reason for the phenomenon of gas dispersal and loss to the surface, the gas chimneys which are detected on seismic records are of the scattered type and not vertical due to the influence of the region by different fault patterns, including transverse faults, which are difficult to accurately diagnose on currently available Seismic data.
5. Laboratory analyzes of soil models at the site of the phenomenon and the surrounding areas indicated a clear discrepancy in the amount of pollution, as the surface models recorded very few percentages compared to the subsurface models that recorded the highest pollution values, especially the two samples at depths (12 and 13) meters (in the well that It was drilled), where the highest values of hydrocarbon pollution were recorded, which indicates that hydrocarbon emissions have subsurface roots and that they are not only caused by surface pollution factors.
6. The results of gas analyze using the Gasmet device indicated that there is a similarity between the nature of the gases emitted in the region of the phenomenon and the gases diagnosed in one of the newly drilled exploratory oil wells, which were measured using the same device.
7. Mig- hydrocarbon emissions from effective source rocks in the region or from potential oil and/or gas deposits in the region is one of the most important causes of fires in Al- Ruhban area and is a direct indication of hydrocarbon presence, which calls for reassessment of the hydrocarbon potential of the region.

Open Access
No. 34 part 2, April 2022, pp. 18-34

P- ISSN: 2220-5381
E- ISSN: 2710-1096

References

[1] Oil Explorations, the file of the promising team to identify exploratory and appraisal wells for Iraq's structures, 2002.

[2] www.globalsecurity.org, the administrative map of Iraq.

[3] Study of Interpretations of Seismic Information for Merjan Fields - West Al Kifl 2D/3D, Oil Exploration Company, 2014.

[4] Fairhead, J.D., A. Salem, L. Cascone, M. Hammill, S. Masterton and E. Samson, “New developments of the magnetic tilt-depth method to improve structural mapping of sedimentary basins”, Geophysical Prospecting, v. 59, p. 1072-1086, 2011.

[5] Peters, K.E., Walters, C.C., Moldowan, J.M., The Biomarker Guide, Volume 2. Biomarkers and Isotopes in Petroleum Exploration and Earth History. Cambridge, Cambridge University Press, 2nd edition, 1155, 2005.

[6] Speight J. G., Natural Gas (Second Edition) A Basic Handbook. ISBN978-0-12-809570-6. Elsevier Inc.P. 462, 2018.